55
Sensing Glucose and Other Metabolites in Skin

Elina A. Genina, Kirill V. Larin, Alexey N. Bashkatov, and Valery V. Tuchin

55.1
Introduction

Recent technological advances in the photonics industry have led to a resurgence of interest in optical imaging technologies and real progress towards the development of noninvasive clinical functional imaging systems. Application of optical methods to physiological condition monitoring and cancer diagnostics, and also for treatment, is a growing field owing to the simplicity, low cost, and low risk of these methods. The development of noninvasive measurement techniques for monitoring of endogenous (metabolic) agents in human tissues is very important for the diagnosis and therapy of various human diseases and might play a key role in the proper management of many devastating conditions.

Glucose is a monosaccharide sugar with chemical formula $C_6H_{12}O_6$. It is one of the most important carbohydrate nutrient sources and is fundamental to almost all biological processes as it required for the production of ATP and other essential cellular components. The normal range of glucose in human blood is 70–160 mg dl^{-1} (3.9–8.9 mM; 1 mM = 18.0 mg dl^{-1}) depending on the time of the last meal, the extent of physical tolerance, and other factors [1]. Freely circulating glucose molecules in the bloodstream stimulate the release of insulin from the pancreas. Insulin (a large peptide hormone composed of two proteins bound together) helps glucose molecules to penetrate the cell wall by binding to specific receptors in cell membranes, which are normally impermeable to glucose. Diabetes is a disorder caused by decreased production of insulin, or by decreased ability to utilize insulin in transport of the glucose across cell membrane. As a result, a high and potentially dangerous concentration of glucose can be accumulated in the blood (hyperglycemia) during the disease [2]. Therefore, it is of great importance to maintain blood glucose concentration within the normal range in order to prevent possibly severe complications.

A significant role for physiological glucose monitoring is in the diagnosis and management of several metabolic diseases, such as diabetes mellitus (or simply diabetes). A number of invasive and noninvasive techniques have been investigated

Handbook of Biophotonics. Vol.2: Photonics for Health Care, First Edition. Edited by Jürgen Popp, Valery V. Tuchin, Arthur Chiou, and Stefan Heinemann.

for glucose monitoring [3]; however, the problem of noninvasive glucose monitoring in a clinically acceptable form has not yet been solved.

While the standard analysis of blood currently involves puncturing a finger and subsequent chemical analysis of collected blood samples, in recent decades noninvasive blood glucose monitoring has become an increasingly important topic of investigation in the realm of biomedical engineering. In particular, the introduction of optical approaches has brought exciting advances to this field [4].

Tissue metabolites play an important role in the state of the human organism. For example, bilirubin-IXα, a metabolite of normal heme degradation, occurs in blood as a water-soluble complex with human serum albumin. It can cause life-threatening neurotoxic effects in babies with hyperbilirubinemia if its level becomes too high and it partitions into the brain [5]. Therefore, noninvasive monitoring of the bilirubin level in serum is very important in some clinical cases.

The defense mechanism of the skin is based on the action of antioxidant substances such as carotenoids, vitamins, and enzymes. β-Carotene and lycopene represent more than 70% of the carotenoids in the human organism. The topical or systemic application of β-carotene and lycopene is the general strategy for improving the defense system of the human body. For the evaluation and optimization of this treatment, it is necessary to measure the β-carotene and lycopene concentrations in the tissue, especially in the human skin as the barrier to the environment [6].

Many optical techniques for sensing different tissue metabolites and glucose in living tissue have been developed over the last 50 years. Methods based on fluorescence [7–17], near-infrared (NIR) and mid-infrared (mid-IR) spectroscopic [18–26], Raman spectroscopic [22, 27–29], photoacoustic [30, 31], optical coherence tomography (OCT) [32–36], and other techniques are discussed in this chapter.

55.2 Light–Tissue Interaction

Optical sensing techniques are defined by light–tissue interaction. This interaction depends on the optical properties of tissue components and structures. The absorption depends on the type of predominant absorption centers and water content in tissues. Absorption for most tissues in the visible region is insignificant except for the absorption bands of blood hemoglobin and some other chromophores [37]. The absorption bands of protein molecules are mainly in the near-ultraviolet (UV) region. Absorption in the IR region is essentially defined by the water absorption spectrum and its concentration in tissues. In the NIR spectral range, the main light absorbers are water and lipids, which are present in different tissues in various quantities. In this spectral range, the absorption bands of water in skin with maxima at 930, 970 [38], 1197, 1430, and 1925 nm [39] and lipids with maxima at 1212, 1710, and 1780 nm [40, 41] are observed. The absorption bands of oxyhemoglobin with maxima at about 415, 540, and 575 nm are observed in the visible spectral range [42, 43]. Absorption of water in this spectral range is negligible.

Fluorescence arises upon light absorption and is related to an electronic transition from the excited state to the ground state of a molecule. Fluorescence spectra often give detailed information on fluorescent molecules, their conformation, binding sites, and interaction within cells and tissues or other molecules. On excitation of biological objects by UV light ($\lambda \leq 370$ nm), autofluorescence of proteins and also of nucleic acids can be observed. Autofluorescence of proteins is related to the amino acids tryptophan, tyrosine, and phenylalanine with absorption maxima at 280, 275, and 257 nm, respectively, and emission maxima between 280 nm (phenylalanine) and 350 nm (tryptophan) [44–47]. Fluorescence from collagen or elastin is excited between 400 and 600 nm with maxima around 400, 430, and 460 nm. Fluorescence of collagen and elastin can be used to distinguish various types of tissues, for example, epithelial and connective tissues [46–49].

The reduced form of coenzyme nicotinamide adenine dinucleotide (NADH) is excited selectively in the wavelength range 330–370 nm. NADH is most concentrated within mitochondria, where it is oxidized within the respiratory chain located within the inner mitochondrial membrane, and its fluorescence is an appropriate parameter for detection of ischemic or neoplastic tissues [46, 49]. Flavin mononucleotide (FMN) and flavin adenine dinucleotide (FAD) with excitation maxima around 380 and 450 nm have also been reported to contribute to intrinsic cellular fluorescence [46].

55.3 Fluorescence Measurements

Fluorescent kinetic probes have been used to obtain information on the antioxidant activity of the skin and eye pigment melanin and its biogenetic precursors 5,6-dihydroxyindole and 5,6-dihydroxyindole-2-carboxylic acid [50]. These constitute the major monomeric building blocks of eumelanin, the brown and dark melanin type. These precursors occur in relatively high local abundance in the melanocytes and keratinocytes, and their enhanced blood or urine levels provide biochemical markers for malignant melanoma and a diagnostic tool for its therapy [50].

Porphyrin molecules, for example, protoporphyrin, coproporphyrin, uroporphyrin, and hematoporphyrin, occur within the biosynthetic pathway of hemoglobin, myoglobin, and cytochromes. Abnormalities in heme synthesis, occurring in cases of porphyries and some hemolytic diseases, may enhance considerably the porphyrin level within tissues [44]. Several bacteria, for example, *Propionibacterium acnes*, and bacteria within dental plaque (biofilm), such as *Porphyromonas gingivalis*, *Prevotella intermedia*, and *Prevotella nigrescens*, accumulate considerable amounts of protoporphyrin [51, 52]. Therefore, acne and oral and tooth lesion detection based on measurements of intrinsic fluorescence specific to porphyrin molecules appears to be a promising method of disease diagnostics. For example, time-gated fluorescence spectroscopy was successfully applied to the detection of the tumor within

tissues based on the strong autofluorescence signal coming from accumulated porphyrins [53].

A number of fluorescence-based techniques have been developed and applied in attempts to sense blood glucose concentration [4, 7–10]. The techniques can be subdivided into two general categories: glucose oxidase (GOx)-based and affinity-binding sensors. Sensors in the first category use the electroenzymatic oxidation of glucose by GOx in order to generate an optically detectable glucose-dependent signal [7]. In the late 1990s, research towards a reagentless glucose sensor, using the deactivated apo-GOx enzyme [8], was started, which used the enzyme as a receptor rather than a catalyst. This work showed that apo-GOx retained its high specificity and in many ways paved the way for advances in the development of a new biosensor genre [9, 10]. Several methods for optical detection of the products of this reaction and, hence, the glucose concentration driving the reaction have been presented [11–13]. A simple approach for creating a sensor based on this reaction is to incorporate an oxygen-sensitive dye such as a ruthenium complex [7, 13]. Ruthenium(II) complexes exhibit fluorescence quenching in the presence of oxygen; therefore, a decrease in local oxygen concentration can be detected as an increase in fluorescence of a ruthenium-based dye. Incorporating GOx and a ruthenium dye together results in a sensor whose fluorescence increases with increase in glucose concentration, since increased glucose concentration will lead to an increased consumption of O_2. A disadvantage of this simple approach is that a decrease in local oxygen content may not be distinguished from a rise in glucose concentration.

Fluorescent affinity-binding sensors utilize competitive binding between glucose and a suitable labeled fluorescent compound to a common receptor site. Several methods are based on Förster resonance energy transfer (FRET) and on competition between glucose and dextran for concanavalin-A (ConA) binding sites [7]. The assay components are ConA labeled with an energy acceptor, or an energy donor, and dextran labeled with the complementary molecule for FRET [14, 15]. Glucose displaces the dextran labeled with the fluorophore at the ConA binding sites and consequently FRET-based quenching occurs as its fluorescence it critically dependent on the distance between donor molecule (e.g., ConA) and acceptor molecule (e.g., dextran). The use of ConA as the membrane-bound molecule affords a very sensitive technique because of the strong affinity of ConA to glucose. Using this approach, glucose concentrations can be measured by a decrease in amplitude of the fluorescence peak with increasing glucose concentration. In either approach, the fluorescence techniques appears to be very specific to glucose and sensitive to glucose concentration, without interference from other constituents frequently found in blood and tissues.

Although no fluorescence-based sensing devices are yet commercially available, it appears that a number of the techniques have been sufficiently developed to expect that clinically-viable devices are just over the horizon, and more activity in trials will be observed in the next few years. Advances in nanomaterials such as quantum dots will likely allow improvements in optical stability and choice of excitation/emission wavelengths for various transduction methods [16, 17].

55.4 IR Spectroscopy

Measurements of the absorption and scattering of NIR light traveling through tissue may provide a useful means to quantify functional parameters of tissues, such as total hemoglobin concentration and blood oxygen saturation and glucose [54]. The optical absorption methods for glucose measurements are based on the concentration-dependent absorption of specific wavelengths of light by glucose or other metabolites. In theory, a beam of radiation may be directed through a blood-containing portion of the body and the exiting light analyzed to determine the content of glucose by assessing the absorption spectrum.

For example, the mid-IR spectral bands of glucose and other carbohydrates have been assigned and are dominated by C−C, C−H, O−H, O−C−H, C−O−H and C−C−H stretching and bending vibrations [22]. The 800–1200 cm^{-1} fingerprint region of the IR spectrum of glucose has bands at 836, 911, 1011, 1047, 1076, and 1250 cm^{-1}, which have been assigned to C−H bending vibrations [22]. A 1026 cm^{-1} band corresponds to a C−O−H bending vibration and the 1033 cm^{-1} band can be associated with the ν(C−O−H) vibration [22] or the ν(C−O−C) vibration [55]. Therefore, it might be possible to utilize these spectrum "fingerprints" to quantify the concentration of carbohydrates in the sample with good specificity.

Despite the specificity offered by IR absorption spectroscopy, its application to quantitative blood glucose measurement is limited. A strong background absorption by water and other components of blood and tissues severely limits the pathlength that may be used for transmission spectroscopy to roughly 100 μm or less. Further, the magnitude of the absorption peaks and the dynamic range required to record them make quantification based on these sharp peaks difficult. Nonetheless, attempts have been made to quantify blood glucose using IR absorption spectroscopy *in vitro* and *in vivo* [8, 23–26].

A new concept for *in vivo* glucose detection in the mid-IR spectral range is based on the use of two quantum cascade lasers emitting at wavelengths 9.26 and 9.38 μm to produce photoacoustic signals in the forearm skin [56]. One of the wavelengths correlates with glucose absorption, whereas the other does not. Determination of glucose concentration in the extracellular fluid of the stratum spinosum permits the deduction of the glucose concentration in blood, because the two factors correlate closely with each other. This method allows one to improve glucose specificity and to remove the effect of other blood substances.

In contrast to the mid-IR range, the incident radiation in the NIR spectral range passes relatively easily through water and body tissues, allowing moderate pathlengths to be used for the measurements. Therefore, a large amount of effort has been devoted to the development of NIR spectroscopic techniques for the noninvasive measurement of blood glucose [18]. The NIR region is ideal for the noninvasive measurement of human body compositions because biological tissue is relatively transparent to light in this region, the so-called therapeutic window. The molecular formula of glucose is $C_6H_{12}O_6$ and several hydroxyl and methyl groups are present.

They are mainly hydrogen functional groups whose absorption occurs in the NIR region. For glucose, the second overtone absorption is in the spectral region 1100–1300 nm and the first overtone absorption is in the region 1500–1800 nm [19]. In the range 1400–1500 nm, there is a peak that corresponds to the absorption peak of water. This information provides the theoretical basis for the measurement of blood glucose using NIR spectroscopy [19, 20].

The concept of noninvasive blood glucose sensing using the scattering properties of blood is an alternative to the spectral absorption method. The method of NIR frequency-domain reflectance is based on changes in glucose concentration, which affect the refractive index mismatch between the interstitial fluid and tissue fibers, and hence reduced scattering coefficient μ'_s [57, 58]. The refractive index n of the interstitial fluid modified by glucose is defined by the equation [44]

$$n_{glw} = n_w + 1.515 \times 10^{-6} \times C_{gl} \tag{55.1}$$

where C_{gl} is glucose concentration in $\mathrm{mg\,dl^{-1}}$ and n_w is the refractive index of water [58]. As the subject's blood glucose rise, μ'_s decreases (see Figure 55.1). Key factors for the success of this approach are the precision of the measurements of the reduced scattering coefficient and the separation of the scattering changes from

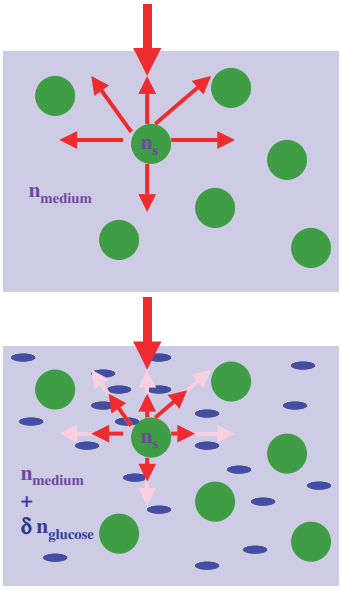

Figure 55.1 Mechanism of glucose-induced changes in the scattering coefficient of a medium: the increase in glucose concentration in the medium (shown as blue ellipses) changes the refractive index of the medium by $+\delta n_{glucose}$, decreases the refractive index mismatch between scattering centers (shown as green circles) and the medium, and, hence, reduces the scattering coefficient (the scattering of light is shown as thin red arrows and incident light is shown as thick red arrows).

absorption changes, as obtained with the NIR frequency-domain spectrometer [57]. Evidently, other physiological effects related to glucose concentration could account for the observed variations of μ'_s and, as it was mentioned earlier, the effect of glucose on the blood flow in the tissue may be one of the sources of the errors in μ'_s measurements.

One critical difficulty associated with *in vivo* blood glucose assay is the extremely low signal-to noise ratio of the glucose peak in the NIR spectrum of human skin tissue. Therefore, the main problem in NIR glucose monitoring is the construction of calibration models [19, 20, 59, 60].

The calibration models typically developed from controlled experiments such as oral glucose tolerance tests might have a better opportunity to provide an acceptable correlation between blood glucose level and the reduced scattering coefficient. At present, the utilization of several experiment data sets for quantitative modeling is most useful to avoid the chance of poor temporal correlation. In one study [59], partial least-squares regression was carried out for the NIR data (total 250 paired data set) and calibration models were built for each subject individually. The selection of informative regions in NIR spectra for analysis can significantly refine the performance of these full-spectrum calibration techniques [60].

A floating-reference method of calibration has been described [20, 21]. The key factor and precondition of the method are the existence of a reference position where diffuse reflectance light is not sensitive to the variations in glucose concentration. Using the signal at the reference position as the internal reference for human body measurement can improve the specification for extraction of glucose information [20].

55.5
Photoacoustic Technique

The photoacoustic technique is based on sensitive time-resolved detection and analysis of laser-induced pressure waves using an ultrasound transducer. Both *in vitro* and *in vivo* studies have been carried out in the spectral range of the transparent "tissue window" around the 1 μm, to assess the feasibility of photoacoustic spectroscopy (PAS) for noninvasive glucose detection [30]. The photoacoustic (PA) signal is obtained by probing the sample with monochromatic radiation, which is modulated or pulsed. Absorption of probe radiation by the sample results in localized short-duration heating. Thermal expansion then gives rise to a pressure wave, which can be detected with a suitable acoustic transducer. An absorption spectrum for the sample can be obtained by recording the amplitude of generated pressure waves as a function of probe beam wavelength [30]. The pulsed PA signal is related to the properties of a turbid medium by the equation [30]

$$PA = k\left(\beta v^n / C_p\right) E_0 \mu_{eff} \tag{55.2}$$

where PA is the signal amplitude, k is a proportionality constant, E_0 is the incident pulse energy, β is the coefficient of volumetric thermal expansion, v is the speed of

sound in the medium, C_p is the specific heat capacity, n is a constant between one and two, depending on the particular experimental conditions, and $\mu_{eff} = \sqrt{3\mu_a(\mu_a + \mu'_s)}$. In the PAS technique, the effect of glucose can be analyzed by detecting changes in the peak-to-peak value of laser-induced pressure waves due to changes in the absorption or scattering as a function of the glucose concentration [31, 61].

Investigations have demonstrated the applicability of PAS to the measurement of glucose concentration [31, 32]. The greatest percentage change in the PA response was observed in region of the C−H second overtone at 1126 nm, with a further peak in the region of the second O−H overtone at 939 nm [30]. In addition, the generated pulsed PA time profile can be analyzed to detect the effect of glucose on tissue scattering, which is reduced by an increase in glucose concentration [62].

Monitoring of the photoisomerization of bilirubin–human serum albumin (BR–HSA) complex is very important in the phototherapy of jaundiced newborns. This complex represents a chromophore–protein interaction. Isomerization reactions of BR–HSA have revealed a detectable structural volume change when studied by photothermal techniques such as laser-induced optoacoustic spectroscopy. The PA signal from solutions of BR–HSA together with the signal amplitude from the calorimetric reference was used to calculate the structural volume change within detection limits [63].

55.6 Raman Spectroscopy

Raman spectroscopy is a powerful technique for the analysis and identification of molecules in a sample. Raman spectroscopy measures inelastically scattered light that results from oscillations and rotations of atoms and atomic groups in molecules (see Figure 55.2). It can provide potentially precise and accurate analysis of metabolite concentrations and biochemical composition. Raman spectra can be utilized to identify molecules because these spectra are characteristic of variations in the molecular polarizability and dipole momentum. Enejder *et al.* [28] accurately measured glucose concentrations in 17 nondiabetic volunteers following an oral glucose tolerance protocol.

β-Carotene and lycopene have different absorption values at 488 and 514.5 nm and, consequently, the Raman lines for β-carotene and lycopene have different scattering efficiencies with 488 and 514.5 nm excitations. These differences were used for the determination of the concentrations of β-carotene and lycopene. The Raman signals are characterized by two prominent Stokes lines at 1160 and 1525 cm^{-1}, which have nearly identical relative intensities [6]. Thus, resonance Raman spectroscopy was used as a fast and noninvasive optical method of measuring the absolute concentrations of β-carotene, lycopene, and other carotenoids in human skin and mucosal tissue [6, 64] and for the determination of the influence of IR radiation on their degradation [65].

In contrast to IR and NIR spectroscopy, Raman spectroscopy has a spectral signature that is less affected by water, which is very important for tissue studies. In addition, Raman spectral bands are considerably narrower (typically

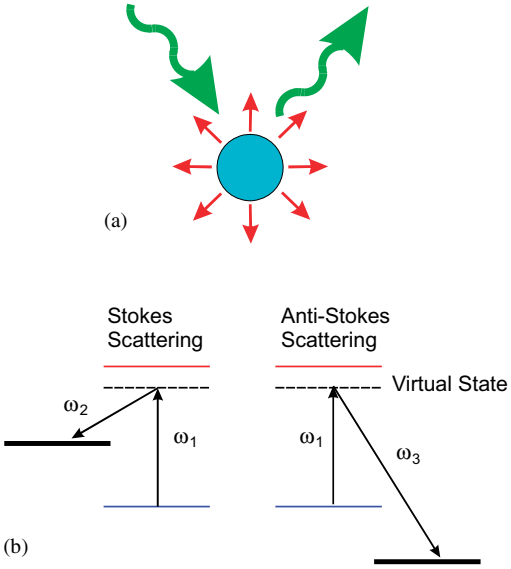

Figure 55.2 Basic principle of Raman spectroscopy: (a) a small portion of photons incident on a target molecule scatters with a shift in photon energy due to molecular vibrations; (b) energy diagram representing the process of Stokes and anti-Stokes scattering (note: there is no transfer of electron population to the "virtual state").

10–20 cm^{-1} [29]) than those produced in NIR spectroscopy. Raman spectroscopy also has the ability for the simultaneous estimation of multiple metabolites, requires minimum sample preparation, and would allow for direct sample analysis [7]. Like IR absorption spectra, Raman spectra exhibit highly specific bands that are dependent on concentration. As a rule, for Raman analysis of tissue, the spectral region between 400 and 2000 cm^{-1}, commonly referred to as the "fingerprint region," is employed.

Different molecular vibrations lead to Raman scattering in this part of the spectrum. In many cases, bands can be assigned to specific molecular vibrations or molecular species, aiding the interpretation of the spectra in terms of biochemical composition of the tissue [7].

Because of the reduction of elastic light scattering on tissue optical clearing, more effective interaction of a probing laser beam with the target molecules is expected. The optical clearing agents increase the signal-to-noise ratio, reduce the systematic error incurred as a result of incompletely resolved surface and subsurface spectra, and significantly improve the Raman signal [66].

55.7 Occlusion Spectroscopy

An approach known as occlusion spectroscopy (OS) was established as a noninvasive method to evoke blood-specific variations of spectral characteristics [67]. The OS

technique is based on the observation that the cessation of blood flow triggers a change in time of the optical characteristics of blood *in vivo*. Because a state of temporary blood flow cessation at the measurement site is created, the average size of aggregates, which are the main scattering centers, begins to grow. Consequently, the mean free path, the light scattering pattern, and the mean absorption coefficients start to evolve with a growth in average size of the scattering particles [68].

The key element of OS is the fact that light scattering changes, originated solely by the blood, drive the optical response of the media. Light scattering fluctuations are associated with both the red blood cells aggregation process and the mismatch of refractive indices of the aggregates and their surrounding media. Glucose present in blood increases the refractive index of plasma and thus decreases the scattering coefficient of blood. Based on a method of parameterization, increased sensitivity to the changes in glucose concentration in blood plasma is achieved [68]. There are still many obstacles in the modeling of aggregation assistance signals in the blood since red blood cells aggregation kinetics vary strongly from subject to subject.

55.8 Reflectance Spectroscopy

The measurement of bilirubin levels in the serum of newborn infants is a very important problem. Hyperbilirubinemia is a common symptom of neonates due to the accumulation of bilirubin in the serum because the liver has not yet developed the enzymes for oxidizing bilirubin for excretion by the kidneys. An optical fiber-based spectrometer has been used for noninvasive monitoring of cutaneous bilirubin (which correlates with serum levels of bilirubin) [69]. It is possible to deduce the bilirubin levels in the skin directly regardless of variations in background scattering, cutaneous melanin, and cutaneous blood content using first principles of optical transport.

The bilirubin absorption adds to the optical density in the region around 480 nm. The bilirubin concentration, C ($\mathrm{mg\,cm^{-3}}$), is related to the absorption coefficient, $\mu_{\mathrm{a.bi1i}}$ ($\mathrm{cm^{-1}}$), by the extinction coefficient, ε [$\mathrm{cm^{-1}\,(mg\,cm^{-3})^{-1}}$]:

$$\mu_{\mathrm{a.bi1i}} = \varepsilon C \tag{55.3}$$

Hence the absorption coefficient $\mu_{\mathrm{a.bi1i}}$ must be deduced in order to specify the amount of bilirubin in the skin. The optical reduced scattering coefficient, μ'_{s}, can be determined by measurement of skin specimens using an integrating sphere spectrophotometer. μ_{a} and μ'_{s} allow the prediction of the reflectance of the skin R and the collection efficiency f [69]. Also, the factor $f_{\mathrm{std}}R_{\mathrm{std}}$ for the Teflon standard has to be determined. The predicted measurement M^* is calculated as $M^* = f^* R$. Then the predicted and measurement values, M^* and M, are compared using a simplex routine and the value of μ_{a} is updated. Iterative cycling of this algorithm converges on a stable deduced value of μ_{a} using the appropriate f^*. This algorithm is applied to each wavelength being considered for analysis. The result is a true absorption spectrum, $\mu_{\mathrm{a}}(\lambda)$, which is then analyzed for the blood and bilirubin content.

This method can be useful to deduce directly the skin bilirubin levels optically without resorting to calibration by a training set of optical versus laboratory serum measurements on some test newborn population [69].

55.9
Polarimetric Technique

The polarimetric technique for blood glucose monitoring utilizes a physical effect such as optical rotation of the polarization plane by glucose molecules. This feature has been used extensively in industry to detect glucose in aqueous solutions. The basic principle of polarimetry is the following: linearly polarized light passing through a medium containing chiral molecules (such as glucose) experiences rotation of a plane of polarization (see Figure 55.3). The degree of this rotation, ϕ, depends on the optical pathlength, L, the concentration of chiral molecules, C, and an intrinsic property of chiral molecules to rotate polarized light, called the specific rotation constant, α:

$$[\phi]^{T}_{\lambda,\mathrm{pH}} = \frac{\alpha}{LC} \tag{55.4}$$

where the subscripts λ and pH and the superscript T indicate dependence of the specific rotation constant on wavelength, pH, and temperature, respectively.

Several groups have tried to utilize this idea to measure glucose concentration in the aqueous humor of the eye [70–73]. A major disadvantage of this method is that glucose-induced changes in the signal are very small and difficult to measure: the angle of rotation for a 1 cm optical pathlength is less than 0.00004° per 1 mg dl^{-1}.

With the exception of transparent ocular tissues, the human body is highly absorbing and scattering in the UV–IR range, and the validity of Eq. (55.4) is questionable. Specifically, (i) light is highly depolarized upon tissue multiple scattering, so even the initial detection of a polarization-preserved signal from which to attempt glucose concentration extraction is a formidable challenge; (ii) the optical pathlength in turbid media is a difficult quantity to define; (iii) other optically active chiral species are present in tissue, thus contributing to the observed optical rotation and hiding/confounding the specific glucose contribution; and (iv) several optical polarization effects occur in tissue simultaneously (e.g., optical rotation, birefringence, absorption, depolarization), contributing to the resultant polarization signals in a complex interrelated way and hindering their unique interpretation [74, 75].

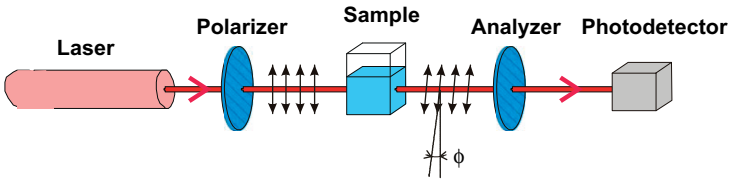

Figure 55.3 Basic principle of the polarimetric approach for glucose monitoring: linearly polarized light passing through a medium containing molecules of glucose experiences rotation of a plane of polarization; ϕ is the degree of this rotation.

Despite these difficulties, it was shown recently that even in the presence of severe depolarization, measurable polarization signals can be obtained reliably from highly scattering media such as biological tissue. Vitkin and co-workers [75] demonstrated surviving linear and circular polarization fractions of light scattered from optically thick turbid media, and measured the resulting optical rotations of the linearly polarized light with the help of a comprehensive turbid polarimetry platform, comprising a highly sensitive experimental system, an accurate forward model that can handle all the complex simultaneous polarization effects manifested by biological tissues, and an inverse signal analysis strategy that can be applied to complex tissue polarimetry data to isolate specific quantities of interest (such as small optical rotation that can be linked to glucose concentration). Additionally, application of this method to relatively transparent tissues (such as the cornea of the human eye) might improve the detection sensitivity of the polarimetric methods [76].

55.10 OCT Technique

An OCT-based method for glucose assessment in tissues has been proposed and its capability for highly sensitive noninvasive monitoring of blood glucose concentration was demonstrated in number of animal and clinical studies [32–35, 77]. The basic principle of this method is to detect and analyze backscattered photons from a tissue layer of interest within the coherence length of a laser source with a two-beam interferometer in the NIR spectral range. OCT technology originates from low-coherence interferometry (a nonscanning/imaging version of OCT) and typically employs a Michelson interferometer, with a broadband laser in the source arm, a beamsplitter, and a photodetector in the detector arm (see Figure 55.4). Light backscattered from the sample is combined with light returned from a mirror in the reference arm of the interferometer, and a photodiode detects the resulting interferometric signal. Interferometric signals can be formed only when the optical pathlength in the sample arm matches the reference arm length within the coherence length of the source. Therefore, by changing the optical pathlength in the reference arm, one-dimensional in-depth profiles of light scattering (A-scans) could be reconstructed in real time with a resolution of about a few microns at depths up to several millimeters.

As mentioned earlier, diffusion of glucose into the interstitial space leads to an increase in the refractive index of the interstitial fluid (ISF), and thus to refractive index matching of collagen fiber (and other tissue components – scatterers) and ISF [64]. Since the scattering coefficient of tissues depends on the refractive index, n, mismatch between ISF and tissue components (fibers, cell components), an increase in tissue glucose concentration will increase the refractive index of the ISF, which will decrease the scattering coefficient of the tissue as a whole. Since the OCT technique measures the in-depth light distribution with high resolution, changes in the in-depth distribution of the tissue scattering coefficient and/or refractive index are reflected in changes in the OCT signal that could be analyzed [32–35, 77].

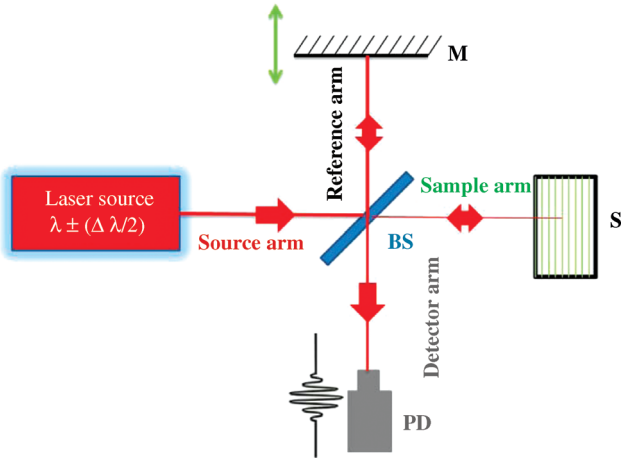

Figure 55.4 General schematic of an OCT system. λ is the central wavelength of the laser source, $\Delta\lambda$ is the bandwidth of the laser source, M is the mirror, S is the sample, BS is the beamsplitter, and PD is the photodetector.

The OCT studies performed in animals (New Zealand white rabbits and Yucatan micropigs) and normal human subjects (during oral glucose tolerance tests) demonstrated (1) capability of the OCT technique to detect changes in scattering coefficient with an accuracy of about 1.5%; (2) a sharp and linear decrease in the OCT signal slope in the dermis with increase in blood glucose concentration; and (3) the accuracy of glucose concentration monitoring may be substantially improved if optimal dimensions of the probed skin area are used [32–35, 77]. The results suggest that the high-resolution OCT technique has a potential for noninvasive, accurate, and continuous glucose monitoring with high sensitivity. However, an OCT method based on analysis of the in-depth amplitude distribution of low-coherent light in skin might have insufficient sensitivity and repeatability and lack of a proper calibration method. Therefore, the development of novel algorithms (e.g., phase-sensitive measurements) and/or combination with other noninvasive sensing modalities are currently being actively investigated by several groups.

55.11 Conclusion

This chapter demonstrates the variety of optical techniques for sensing glucose and other metabolites in skin. Significant efforts have been made by numerous groups and companies in the past two decades to develop a biosensor for noninvasive blood glucose analysis. These approaches include NIR absorption and scattering, polarimetry, Raman spectroscopy, photoacoustics and OCT. The ability of these techniques to assess blood glucose and other metabolites concentration is summarized in Table 55.1.

Table 55.1 Optical techniques for sensing glucose and other metabolites.

Method	Ability	Ref.
Fluorescent glucose-oxidase based sensors	Use the electroenzymatic oxidation of glucose alone or in combination with oxygen-sensitive dye. Fluorescence of the sensor increases with increase in glucose concentration. Sensitivity to decrease in O_2	[7–13]
Fluorescent affinity-binding sensors	Use binding between agent and a labeled fluorescent compound. Fluorescence of the sensor increases with increase in glucose concentration. Specificity to glucose	[14, 15]
NIR absorption spectroscopy	Uses absorption spectral fingerprints of glucose in "therapeutic window." Low sensitivity of agent concentration measurement in physiologic range	[19, 20]
NIR scattering spectroscopy	Use of the change in reduced scattering coefficient with blood glucose concentration due to matching effect. Sensitivity to other physiological effects related to glucose increase	[57, 58]
Mid-IR spectroscopy	Uses spectrum "fingerprints" to quantify the concentration of carbohydrates in tissue with good specificity	[22–26]
Raman spectroscopy	Uses specific spectral bands that are less affected by water. Provides potentially precise and accurate analysis of metabolite concentration. However, it is difficult to isolate glucose from the background spectrum caused by other tissue components	[6, 28, 64, 65]
Occlusion spectroscopy	Uses light scattering fluctuations, originated by the blood. Sensitivity to the changes in glucose concentration in blood plasma	[67, 68]
Reflectance spectroscopy	Uses optical measurements of body composition. Allows noninvasive estimation of cutaneous bilirubin concentration	[69]
Photoacoustic technique	Uses absorption of probe radiation by the sample that results in localized short-duration heating and then gives rise to a pressure wave, which can be detected with a transducer. Sensitivity to the changes in tissue glucose concentration and bilirubin structural volume	[30–32, 63]
Polarimetry technique	Uses optical rotation of the polarization plane by glucose molecules. Measurable polarization signals can be obtained from highly scattering media such as biological tissue. A major disadvantage is that glucose-induced changes in the signal are very small and difficult to measure: the angle of rotation for a 1 cm optical pathlength is less than 0.00004° per 1 mg dl^{-1}	[70–75]
OCT technique	Uses backscattered photons from a tissue of interest within the coherence length of the laser source with a two-beam interferometer in the NIR spectral range. Sensitivity to the changes in blood glucose concentration. Requires proper calibration	[32–35, 77]

Despite significant efforts, the described techniques for noninvasive monitoring of glucose concentration have faced limitations associated with low sensitivity and accuracy and insufficient specificity of glucose concentration measurement in the physiologic range. Therefore, further development of the methods is important for noninvasive diagnosis of various human diseases and blood glucose monitoring and is the subject of current research efforts by several groups.

Acknowledgments

This work was supported in part by the following: 224 014 Photonics4life-FP7-ICT-2007-2; RUB1-2932-SR-08 CRDF; Russian Federation Ministry of Science and Education 2.1.1/4989 and 2.2.1.1/2950, Project 1.4.09 of Federal Agency of Education of the Russian Federation; RFBR-08-02-92224-NNSF_a (Russian Federation–China); RFBR-10-02-90039-Bel_a; and Russian Federation governmental contracts 02.740.11.0770 and 02.740.11.0879.

References

1 Goldstein, D.E., Little, R.R., Lorenz, R.A., Malone, J.I., Nathan, D., Peterson, C.M., and Sacks, D.B. (2004) Tests of glycemia in diabetes. *Diabetes Care*, **27**, 1761–1773.

2 Diabetes Control and Complications Trial Research Group (1997) Hypoglycemia in the diabetes control and complications trial. *Diabetes*, **46**, 271–286.

3 Tuchin, V.V. (ed.) (2009) *Handbook of Optical Sensing of Glucose in Biological Fluids and Tissues*, Taylor & Francis/CRC Press, Boca Raton, FL.

4 Klonoff, D.C. (2005) Continuous glucose monitoring. *Diabetes Care*, **28**, 1231–1239.

5 Williams, R.M., McDonagh, A.F., and Braslavsky, S.E. (1998) Structural volume changes upon photoisomerization of the bilirubin–albumin complex: a laser-induced optoacoustic study. *Photochem. Photobiol.*, **68** (4), 433–437.

6 Darvin, M.E., Gersonde, I., Meinke, M., Sterry, W., and Lademann, J. (2005) Non-invasive *in vivo* determination of the carotenoids beta-carotene and lycopene concentrations in the human skin using the Raman spectroscopic method. *J. Phys. D Appl. Phys.*, **38**, 2696–2700.

7 McNichols, R.J. and Cote, G.L. (2000) Optical glucose sensing in biological fluids: an overview. *J. Biomed. Opt.*, **5**, 5–16.

8 D'Auria, S., Herman, P., Rossi, M., and Lakowicz, J.R. (1999) The fluorescence emission of the apo-glucose oxidase from *Aspergillus niger* as probe to estimate glucose concentrations. *Biochem. Biophys. Res. Commun.*, **263**, 550–553.

9 Mack, A.C., Mao, J., and McShane, M.J. (2005) Transduction of pH and glucose-sensitive hydrogel swelling through fluorescence resonance energy transfer, in *Sensors, 2005 IEEE Conference*, IEEE, (ed. A. Shkel), University of California, Irvine, CA, USA, pp. 912–916.

10 Chinnayelka, S. and McShane, M.J. (2005) Microcapsule biosensors using competitive binding resonance energy transfer assays based on apoenzymes. *Anal. Chem.*, **77**, 5501–5511.

11 Moreno-Bondi, M.C., Wolfbeis, O.S., Leiner, M.J., and Schaffar, B.P.H. (1990) Oxygen optrode for use in a fiber-optic glucose biosensor. *Anal. Chem.*, **62**, 2377–2380.

12 Rosenzweig, Z. and Kopelman, R. (1996) Analytical properties and sensor size effects of a micrometer-sized optical fiber glucose biosensor. *Anal. Chem.*, **68**, 1408–1413.

13 Li, L. and Walt, D.R. (1995) Dual-analyte fiber-optic sensor for the simultaneous and continuous measurement of glucose and oxygen. *Anal. Chem.*, **67**, 3746–3752.

14 McCartney, L.J., Pickup, J.C., Rolinski, O.J., and Birch, D.J.S. (2001) Near-infrared fluorescence lifetime assay for serum glucose based on allophycocyanin-labeled concanavalin A. *Anal. Biochem.*, **292**, 216–221.

15 Rolinski, O.J., Birch, D.J.S., McCartney, L.J., and Pickup, J.C. (2001) Fluorescence nanotomography using resonance energy transfer: demonstration with a protein–sugar complex. *Phys. Med. Biol.*, **46**, N221–N226.

16 Coté, G.L. and McShane, M. (2009) Fluorescence-based glucose biosensors, in *Handbook of Optical Sensing of Glucose in Biological Fluids and Tissues* (ed. V.V. Tuchin), Taylor & Francis/CRC Press, Boca Raton, FL, pp. 331–364.

17 Cordes, D.B., Gamsey, S., and Singaram, B. (2006) Fluorescent quantum dots with boronic acid substituted viologens to sense glucose in aqueous solution. *Angew. Chem. Int. Ed.*, **45**, 3829–3832.

18 Marbach, R., Koschinsky, Th., Gries, F.A., and Heise, H.M. (1993) Noninvasive blood glucose assay by near-infrared diffuse reflectance spectroscopy of the human inner lip. *Appl. Spectrosc.*, **47**, 875–881.

19 Heise, H.M., Lampen, P., and Marbach, R. (2009) Near-infrared reflection spectroscopy for non-invasive monitoring of glucose – established and novel strategies for multivariate calibration, in *Handbook of Optical Sensing of Glucose in Biological Fluids and Tissues* (ed. V.V. Tuchin), Taylor & Francis/CRC Press, Boca Raton, FL, pp. 115–156.

20 Xu, K. and Wang, R.K. (2009) Challenges and countermeasures in NIR non-invasive blood glucose monitoring, in *Handbook of Optical Sensing of Glucose in Biological Fluids and Tissues* (ed. V.V. Tuchin), Taylor & Francis/CRC Press, Boca Raton, FL, pp. 281–316.

21 Luo, Y., An, L., and Xu, K. (2006) Discussion on floating-reference method for noninvasive measurement of blood glucose with near-infrared spectroscopy. *Proc. SPIE*, **6094**, 60940K.

22 Vasko, P.D., Blackwell, J., and Koenig, J.L. (1971) Infrared and Raman spectroscopy of carbohydrates. I: Identification of O−H and C−H vibrational modes for D-glucose, malose, cellobiose, and dextran by deuterium substitution methods. *Carbohydr. Res.*, **19**, 297–310.

23 Hahn, S. and Yoon, G. (2006) Identification of pure component spectra by independent component analysis in glucose prediction based on mid-infrared spectroscopy. *Appl. Opt.*, **45**, 8374–8380.

24 Kim, Y.J., Hahn, S., and Yoon, G. (2003) Determination of glucose in whole blood samples by mid-infrared spectroscopy. *Appl. Opt.*, **42**, 745–749.

25 Martin, W.B., Mirov, W.B., and Venugopalan, R. (2002) Using two discrete frequencies within the middle infrared to quantitatively determine glucose in serum. *J. Biomed. Opt.*, **7**, 613–617.

26 Shen, Y.C., Davies, A.G., Linfield, E.H., Elsey, T.S., Taday, P.F., and Arnone, D.D. (2003) The use of Fourier-transform infrared spectroscopy for the quantitative determination of glucose concentration in whole blood. *Phys. Med. Biol.*, **48**, 2023–2032.

27 Yaroslavskaya, A.N., Yaroslavsky, I.V., Otto, C., Puppels, G.J., Guindam, H., Vrensen, G.F.J.M., Greve, J., and Tuchin, V.V. (1998) Water exchange in human eye lens monitored by confocal Raman microspectroscopy. *Biophysics*, **43**, 109–114.

28 Enejder, A.M.K., Scecina, T.G., Oh, J., Hunter, M., Shih, W.-C., Sasic, S., Horowitz, G.L., and Feld, M.S. (2005) Raman spectroscopy for noninvasive glucose measurements. *J.Biomed. Opt.*, **10**, 031114.

29 Hanlon, E.B., Manoharan, R., Koo, T.W., Shafer, K.E., Motz, J.T., Fitzmaurice, M., Kramer, J.R., Itzkan, I., Dasari, R.R., and Feld, M.S. (2000) Prospects for *in vivo* Raman spectroscopy. *Phys. Med. Biol.*, **45**, R1–R59.

30 MacKenzie, H.A., Ashton, H.S., Spiers, S., Shen, Y., Freeborn, S.S., Hannigan, J., Lindberg, J., and Rae, P. (1999) Advances in photoacoustic noninvasive glucose testing. *Clin. Chem.*, **45**, 1587–1595.

31 Kinnunen, M. and Myllyla, R. (2005) Effect of glucose on photoacoustic signals at the

wavelengths of 1064 and 532 nm in pig blood and intralipid. *J. Phys. D Appl. Phys.*, **38**, 2654–2661.

32 Kinnunen, M., Myllylä, R., Jokela, T., and Vainio, S. (2006) *In vitro* studies toward noninvasive glucose monitoring with optical coherence tomography. *Appl. Opt.*, **45**, 2251–2260.

33 Larin, K.V., Eledrisi, M.S., Motamedi, M., and Esenaliev, R.O. (2002) Noninvasive blood glucose monitoring with optical coherence tomography. *Diabetes Care*, **25**, 2263–2267.

34 Esenaliev, R.O., Larin, K.V., Larina, I.V., and Motamedi, M. (2001) Noninvasive monitoring of glucose concentration with optical coherence tomography. *Opt. Lett.*, **26**, 992–994.

35 Larin, K.V., Akkin, T., Esenaliev, R.O., Motamedi, M., and Milner, T.E. (2004) Phase-sensitive optical low-coherence reflectometry for the detection of analyte concentrations. *Appl. Opt.*, **43**, 3408–3414.

36 Esenaliev, R.O. and Prough, D.S. (2009) Noninvasive monitoring of glucose concentration with optical coherence tomography, in *Handbook of Optical Sensing of Glucose in Biological Fluids and Tissues* (ed. V.V. Tuchin), Taylor & Francis/CRC Press, Boca Raton, FL, pp. 563–586.

37 Young, A.R. (1997) Chromophores in human skin. *Phys. Med. Biol.*, **42**, 789–802.

38 McBride, T.O., Pogue, B.W., Poplack, S., Soho, S., Wells, W.A., Jiang, S., Osterberg, U.L., and Paulsen, K.D. (2002) Multispectral near-infrared tomography: a case study in compensating for water and lipid content in hemoglobin imaging of the breast. *J. Biomed. Opt.*, **7**, 72–79.

39 Palmer, K.F. and Williams, D. (1974) Optical properties of water in the near infrared. *J. Opt. Soc. Am.*, **64**, 1107–1110.

40 Martin, K.A. (1993) Direct measurement of moisture in skin by NIR spectroscopy. *J. Soc. Cosmet. Chem.*, **44**, 249–261.

41 Lauridsen, R.K., Everland, H., Nielsen, L.F., Engelsen, S.B., and Norgaard, L. (2003) Exploratory multivariate spectroscopic study on human skin. *Skin Res. Technol.*, **9**, 137–146.

42 Bashkatov, A.N., Genina, E.A., Kochubey, V.I., and Tuchin, V.V. (2005) Optical properties of human skin, subcutaneous and mucous tissues in the wavelength range from 400 to 2000 nm. *J. Phys. D Appl. Phys.*, **38**, 2543–2555.

43 Prahl, S.A. Optical Absorption of Hemoglobin, http://omlc.ogi.edu/spectra/hemoglobin/index.html, Oregon Medical Laser Center, Portland, OR (last accessed 20 December 2010).

44 Tuchin, V.V. (2007) *Tissue Optics: Light Scattering Methods and Instruments for Medical Diagnosis*, SPIE Press, Bellingham, WA.

45 Lakowicz, J.R. (1999) *Principles of Fluorescence Spectroscopy*, 2nd edn, Kluwer Academic/Plenum, New York.

46 Schneckenburger, H., Steiner, R., Strauss, W., Stock, K., and Sailer, R. (2002) Fluorescence technologies in biomedical diagnostics, in *Optical Biomedical Diagnostics* (ed. V.V. Tuchin), vol. **PM107**, SPIE Press, Bellingham, WA, pp. 827–874.

47 Sinichkin, Yu.P., Kollias, N., Zonios, G., Utz, S.R., and Tuchin, V.V. (2002) Reflectance and fluorescence spectroscopy of human skin *in vivo*, in *Optical Biomedical Diagnostics* (ed. V.V. Tuchin), vol. **PM107**, SPIE Press, Bellingham, WA, pp. 725–785.

48 Zhadin, N.N. and Alfano, R.R. (1998) Correction of the internal absorption effect in fluorescence emission and excitation spectra from absorbing and highly scattering media: theory and experiment. *J. Biomed. Opt.*, **3** (2), 171–186.

49 Drezek, R., Sokolov, K., Utzinger, U., Boiko, I., Malpica, A., Follen, M., and Richards-Kortum, R. (2001) Understanding the contributions of NADH and collagen to cervical tissue fluorescence spectra: modeling, measurements, and implications. *J. Biomed. Opt.*, **6** (4), 385–396.

50 Zhang, X., Erb, C., Flammer, J., and Nau, W.M. (2000) Absolute rate constants for the quenching of reactive excited states by melanin and related 5,6-dihydroxyindole metabolites: implications for their antioxidant activity. *Photochem. Photobiol.*, **71** (5), 524–533.

51 Lucchina, L.C., Kollias, N., Gillies, R., Phillips, S.B., Muccini, J.A., Stiller, M.J., Trancik, R.J., and Drake, L.A. (1996) Fluorescence photography in the

evaluation of acne. *J. Am. Acad. Dermatol.*, **35**, 58–63.

52 Soukos, N.S., Som, S., Abernethy, A.D., Ruggiero, K., Dunham, J., Lee, C., Doukas, A.G., and Goodson, J.M. (2005) Phototargeting oral black-pigmented bacteria. *Antimicrob. Agents Chemother.*, **49**, 1391–1396.

53 Schneckenburger, H., Steiner, R., Strauss, W., Stock, K., and Sailer, R. (2002) Fluorescence technologies in biomedical diagnostics, in *Optical Biomedical Diagnostics* (ed. V.V. Tuchin), SPIE Press, Bellingham, WA, pp. 825–874.

54 Cheng F X., Mao, J.-M., Bush, R., Kopans, D.B., Moore, R.H., and Chorlton, M. (2003) Breast cancer detection by mapping hemoglobin concentration and oxygen saturation. *Appl. Opt.*, **42** (31), 6412–6421.

55 Petibois, C., Rigalleau, V., Melin, A.-M., Perromat, A., Cazorla, G., Gin, H., and Deleris, G. (1999) Determination of glucose in dried serum samples by Fourier-transform infrared spectroscopy. *Clin. Chem.*, **45**, 1530–1535.

56 Von Lilienfeld-Toal, H., Weidenmuller, M., Xhelaj, A., and Mantele, W. (2005) A novel approach to non-invasive glucose measurement by mid-infrared spectroscopy: the combination of quantum cascade lasers (QCL) and photoacoustic detection. *Vibr. Spectrosc.*, **38**, 209–215.

57 Maier, J.S., Walker, S.A., Fantini, S., Franceschini, M.A., and Gratton, E. (1994) Possible correlation between blood glucose concentration and the reduced scattering coefficient of tissues in the near infrared. *Opt. Lett.*, **19**, 2062–2064.

58 Kohl, M., Esseupreis, M., and Cope, M. (1995) The influence of glucose concentration upon the transport of light in tissue-simulating phantoms. *Phys. Med. Biol.*, **40**, 1267–1287.

59 Maruo, K., Tsurugi, M., Tamura, M., and Ozaki, Y. (2003) *In vivo* nondestructive measurement of blood glucose by near-infrared diffuse-reflectance spectroscopy. *Appl. Spectrosc.*, **57**, 1236–1244.

60 Jiang, J.H., Berry, R.J., Siesler, H.W., and Ozaki, Y. (2002) Wavelength interval selection in multicomponent spectral analysis by moving window partial least-squared regression with applications to mid-infrared and near-infrared spectroscopic data. *Anal. Chem.*, **74**, 3555–3565.

61 Larin, K.V. and Oraevsky, A.A. (1999) Optoacoustic signal profiles for monitoring glucose concentration in turbid media. *Proc. SPIE*, **3726**, 576–583.

62 Tuchin, V.V. (2006) *Optical Clearing of Tissues and Blood*, SPIE Press, vol. **PM154**, Bellingham, WA,.

63 Williams, R.M., McDonagh, A.F., and Braslavsky, S.E. (1998) Structural volume changes upon photoisomerization of the bilirubin-albumin complex: a laser-induced optoacoustic study. *Photochem. Photobiol.*, **68** (4), 433–437.

64 Ermakov, I.V., Sharifzadeh, M., Ermakova, M., and Gellermann, W. (2005) Resonance Raman detection of carotenoid antioxidants in living human tissue. *J. Biomed. Opt.*, **10** (6), 064028.

65 Darvin, M.E., Gersonde, I., Albrecht, H., Zastrow, L., Sterry, W., and Lademann, J. (2007) *In vivo* Raman spectroscopic analysis of the influence of IR radiation on the carotenoid antioxidant substances beta-carotene and lycopene in the human skin. Formation of free radicals. *Laser Phys. Lett.*, **4** (4), 318–321.

66 Schulmerich, M.V., Cole, J.H., Dooley, K.A., Morris, M.D., Kreider, J.M., and Goldstein, S.A. (2008) Optical clearing in transcutaneous Raman spectroscopy of murine cortical bone tissue. *J. Biomed. Opt.*, **13** (2), 021108.

67 Fine, I. (2002) Non-invasive method and system of optical measurements for determining the concentration of a substance in blood. U.S. Patent US 6400972.

68 Fine, I. (2009) Glucose correlation with light scattering patterns, in *Handbook of Optical Sensing of Glucose in Biological Fluids and Tissues* (ed. V.V. Tuchin), Taylor & Francis/CRC Press, Boca Raton, FL, pp. 250–292.

69 Jacques, S.L., Saidi, I., Ladner, A., and Oelberg, D. (1997) Developing an optical fiber reflectance spectrometer to monitor bilirubinemia in neonates. *Proc. SPIE*, **2975**, 115–124.

70 Cameron, B.D., Gorde, H.W., Satheesan, B., and Coté, G.L. (1999) The use of polarized laser light through the eye for

noninvasive glucose monitoring. *Diabetes Technol. Ther.*, **1**, 135–143.

71 Cameron, B.D. and Anumula, H. (2006) Development of a real-time corneal birefringence compensated glucose sensing polarimeter. *Diabetes Technol. Ther.*, **8**, 156–164.

72 Pu, C., Zhu, Z., and Lo, Y.H. (2000) A surface-micromachined optical self-homodyne polarimetric sensor for noninvasive glucose monitoring. *IEEE Photon. Technol. Lett.*, **12**, 190–192.

73 Ansari, R.R., Boeckle, S., and Rovati, L. (2004) New optical scheme for a polarimetric-based glucose sensor. *J. Biomed. Opt.*, **9**, 103–115.

74 Wood, M.F.G., Guo, X., and Vitkin, I.A. (2007) Polarized light propagation in multiply scattering media exhibiting both linear birefringence and optical activity: Monte Carlo model and experimental methodology. *J. Biomed. Opt.*, **12**, 014029.

75 Wood, M.F.G., Ghosh, N., Guo, X., and Vitkin, I.A. (2009) Towards noninvasive glucose sensing using polarization analysis of multiply scattered light, in *Handbook of Optical Sensing of Glucose in Biological Fluids and Tissues* (ed. V.V. Tuchin), Taylor & Francis/CRC Press, Boca Raton, FL, pp. 536–574.

76 Malik, B.H. and Coté, G.L. (2010) Real-time, closed-loop dual-wavelength optical polarimetry for glucose monitoring. *J. Biomed. Opt.*, **15** (1), 017002.

77 Larin, K.V., Motamedi, M., Ashitkov, T.V., and Esenaliev, R.O. (2003) Specificity of noninvasive blood glucose sensing using optical coherence tomography technique: a pilot study. *Phys. Med. Biol.*, **48**, 1371–1390.